doi.org/10.36721/PJPS.2023.36.5.SP.1627-1635.1

Development and characterization of letrozole-encapsulated polymeric beads for sustained release

Muhammad Abu Sufian[1], Syed Atif Raza[2], Humayun Riaz[3], Waqas Ahmad[4*], Zia Mohy Uddin Khan[3], Hammad Yousuf[3], Muhammad Affan[3], Ayesha Ghafoor[2], Adeel Masood Butt[5], Umar Farooq[6] and Wajeeha Akram[1]

[1]Department of Pharmaceutics, Faculty of Pharmaceutical Sciences, Government College University, Faisalabad, Pakistan
[2]University College of Pharmacy, University of the Punjab, Lahore, Pakistan
[3]Rashid Latif College of Pharmacy, Rashid Latif Khan University, Lahore, Pakistan
[4]Faculty of Pharmaceutical Sciences, The University of Lahore, Lahore, Pakistan
[5]Institute of Pharmaceutical Sciences, University of Veterinary & Animal Sciences, Lahore, Pakistan
[6]Faculty of Pharmacy, Grand Asian University, Sialkot, Pakistan

Abstract: The study aimed to prepare and characterize biodegradable sustained-release beads of letrozole (LTZ) for treating cancerous disease. The ionotropic gelation method was used for the preparation and calcium chloride ($CaCl_2$) was used as a gelating agent, while chitosan (CTS) and sodium alginate (NaAlg) as biodegradable polymeric matrices in the blend hydrogel beads. The beads were characterized for their size, surface morphology, drug entrapment efficiency, drug-polymer interaction, and crystallinity using different analytic techniques, including optical microscopy, Scanning Electron Microscopy (SEM), UV-spectroscopy, Fourier-transform Infrared Spectroscopy (FTIR), Thermogravimetric Analysis (TGA), Differential Scanning Calorimetry (DSC) and X-ray Diffraction Analysis (XRD) respectively. *In vitro* swelling studies were also applied to observe the response of these polymeric networks against different pH (at 1.2, 6.8, and 7.4 pH). The results from TGA and DSC exhibited that the components in the formulation possess better thermal stability. The XRD of polymeric networks displays a minor crystalline and significant amorphous nature. The SEM micrographs revealed that polymeric networks have uneven surfaces and grooves. Better swelling and *in vitro* outcomes were achieved at a high pH (6.8,7.4), which endorsed the pH-responsive characteristics of the prepared beads. Hence, beads based on chitosan and sodium alginate were successfully synthesized and can be used for the controlled release of letrozole.

Keywords: Letrozole, sustained release, chitosan, sodium alginate, chemotherapy.

INTRODUCTION

Drug delivery through polymeric systems has played a fundamental role due to their versatile properties and ability to be customized for specific applications. Among them, biodegradable polymers are foremost owing to their biocompatibility and biodegradability (Daniel, 2021). Several benefits can be achieved by entrapping drugs in a delivery system. The embedding into a delivery system can shelter a drug from degradation, enhance its stability, and control its release kinetics over an extended period (Zaidi and Cherif, 2019). This controlled release can be achieved through various mechanisms, including diffusion, erosion, or a combination (Školakova *et al.,* 2019). Besides, a drug delivery system can be functionalized to supply a drug to a specific site or cell within the body (Yetisgin *et al.,* 2020). Hence, this targeting approach favors improved drug efficacy while abating side effects on healthy tissue. Particularly for polymeric beads, their advantage over the other delivery systems is that their size and shape can be precisely controlled based on the target site or specific therapeutic needs. For instance, smaller beads can be used for intravenous delivery, while larger ones may be suitable for implantation.

Cancer is the leading cause of death worldwide. Among them, breast cancer is one of the most prevalent and leading causes of death in women worldwide (Zaidi and Cherif, 2019). Breast cancer metastasis ensues in as high as 40% of patients with primary breast cancer. The major cause of breast cancer is hormone-dependent and the critical mediator hormone for its progression and metastasis is estrogen. Unfortunately, the prognosis of the cancer is still poor, although systemic chemotherapy, molecular targeted therapy and hormonal therapy are widely practiced as standard clinical treatments for breast cancer (Hosonaga *et al.,* 2020). Breast cancer metastasis to the hilum and mediastinum may cause life-threatening conditions, such as hemoptysis, bronchial infiltration, and superior vena cava syndrome (Bailleux *et al.,* 2021). To evade breast tumour metastasis, clinician expects to discover optimal therapies that persuade rapid tumor shrinkage. Albeit, the alternative treatment, lobectomy, is associated with intense invasive procedures and high mortality (Hakan *et al.,* 2019; Kim *et al.,* 2019). Among

*Corresponding author: e-mail: waqas.ahmad@pharm.uol.edu.pk

the novel therapies, transcatheter arterial chemoembolization (TACE) became a popular approach for cancer therapy, mainly hepatocellular carcinoma (Shao *et al.,* 2021). In this targeted treatment with a minimally invasive procedure, some advanced tumors (e.g., pulmonary, hepatic, and breast cancer) have been successfully treated with good treatment tolerance (Kennoki *et al.,* 2017). The primary aim of TACE is to occulate the arterial blood supply to tumor tissue and thus synergistically achieve localized chemotherapy to alleviate the side effects of an anticancer drug on surrounding healthy tissue.

Letrozole is a non-steroidal anticancer drug with a hydrophobic nature and is generally used for estrogen-dependent breast cancer in postmenopausal women. It inhibits estrogen biosynthesis within the body, making it an effective therapy for estrogen-induced breast cancer (Gnant *et al.,* 2021, Sood *et al.,* 2021). Letrozole, along with other aromatase inhibitors, possesses many adverse effects like hypercholesterolemia, arthralgia, bone damage and fractures, hot flushes and cardiac failure. The drug is immediately transformed into its metabolite, thus owning a short biological half-life. Hence, there is a need to formulate a system/dosage form of letrozole that delivers the drug at a steady rate in the plasma to provide the drug locally to the breast tissues to inhibit the estrogen concentration in the plasma. Generally, developing a novel drug delivery system ensures technological advances and guarantees innovative solutions to old problems. For that purpose, letrozole-loaded beads were developed. CTS and NaAlg are used as a polymer because of their high biodegradability and biocompatibility properties and can also sustain the drug for a longer duration (Lv *et al.,* 2023, Qureshi *et al.,* 2020). One of the common properties of the polymers is their strong bio-adhesiveness with negatively charged mucosal membranes; thus, they enhance the transport of polar drugs across epithelial surfaces. In addition, they are biocompatible and recyclable. Recently, an overwhelming number of researchers have established the efficacy of chemotherapeutic-loaded hydrogels as local drug delivery against many in vitro tumor models after assessing their biocompatibility (Nieto *et al.,* 2022, luca *et al.,* 2023).

This work investigated the effect of a blend of biocompatible and biodegradable polymers; CTS and NaAlg, on loading capacity and release kinetics of a poorly soluble anticancer drug, Letrozole. The drug is a low molecular weight compound (MW 285.3 g/mol) and highly permeates commonly used matrix excipients. To overcome this limitation, cross-linking of biodegradable polymers has already been exhibited to restrict the escape of lower molecular weight drugs, hence offering their sustained release (Song *et al.,* 2018). Another problem related to commonly used synthetic cross-linking agent (e.g., glutaraldehyde, ethylene glycol diglycidyl ether, *N*,*N*′-methylenebisacrylamide, poly (ethylene glycol) diacrylates, epichlorohydrin) is their health concerns and they can cause undesirable effects including irritation to mucosal membranes (Bialik-Wąs *et al.,* 2021). Being low toxic to humans, the use of $CaCl_2$ as a cross-linking agent has been documented in recent studies (Che Nan *et al.,* 2019; Tuan Mohamood *et al.,* 2021). Here, hydrogel beads were prepared by the ionotropic cross-linking method and were characterized using FTIR, XRD, DSC, and SEM to probe the drug-polymer interactions and nature of the drug in the formulations. Also, since the tumor microenvironment often possesses a lower pH level due to the production of lactic acid (5.5-7.2) compared to normal tissue (Boedtkjer and Pedersen, 2020), pH-sensitive hydrogel beads were aimed here. Finally, the release pattern of the drug from the beads was assessed by applying the different kinetic models.

MATERIALS AND METHODS

LTZ was kindly provided by Lianyungang Guike Pharmaceutical China. Low molecular weight chitosan (CAS No. 9012-76-4) (MW 50000Da) was obtained by Sigma-Aldrich (St. Louis, MO, USA), Sodium alginate ($MW=1.93\times10^5$g/mol) was obtained from Daejung Chemical & Metals Co. (China), $CaCl_2$ (CAS No. 10042-42-3) obtained from Daejung chemical & metals co. (China), acetic acid obtained from Tianjin Kermel Chemical Reagents Co. (China). All other chemicals and reagents were of analytical grade.

Preparation of calcium chloride cross-linked blend gel beads

Drug-loaded beads were synthesized by ionotropic cross-linking method using different concentrations of CTS and NaAlg. A final concentration of 2% (w/v) of the polymers was made using various proportions of the polymers (table 1). For this purpose, NaAlg was dissolved in distilled water at 40^{o}C under mechanical stirring. After that, chitosan was added to the sodium alginate solution and mixed thoroughly. In sufficient quantity, acetic acid was added to this solution to dissolve the chitosan in the mixture. Afterward, the pH of the solution was adjusted to 5 by sodium hydroxide (0.1mol/L). A homogeneous blend solution of the two polymers was formed under mechanical stirring at 40^{o}C. In the next step, this solution was added drop wise by a 21-gauge (21G) needle into the 2% (w/v) $CaCl_2$ solution. Smooth and spherical beads formed and placed in the $CaCl_2$ solution for 15-20 minutes. At the end beads were collected and washed three times with distilled water and were placed in an oven at 40^{o}C for 24 hours for the complete drying. To prepare drug-loaded beads, 10% (w/w) of the drug to the total weight of the chitosan and sodium alginate was dissolved in 5mL of methanol and then added to the homogeneous mixture of the polymers. The other processes were the same for the cross linking by $CaCl_2$.

The percentage yield (% w/w) was determined by dividing the weight of the dried beads by the initial dry weight of the starting materials multiplied by a hundred, i.e.,

Characterization

Size determination

An optical microscope was used to measure the size of the beads. The optical microscope was calibrated using the optical micrometer fitted into the eyepiece and a stage micrometer. One division of the stage micrometer was equal to 10µm, and the one division of the ocular micrometer was equal to 2.22×10µm. The size of 10 beads of each formulation was measured, and the average size of each formulation was calculated by adding all the sizes and dividing them by 10.

Drug loading and encapsulation efficiency

The direct method was used to determine entrapment efficiency (EE, %). To measure it and the drug loading (DL, %), 10mg of beads was placed in the 10mL phosphate buffer of pH 7.4 and then stirred on the magnetic stirrer at 100 rotations per minute (rpm) for 48 hours. After that, the remaining beads in the buffer were crushed by the pestle and mortar and then centrifuged at 6000rpm for 30minutes. Then, the spectrophotometer (UV mini 1240, Shimadzu Company, Japan) quantitatively estimated the drug in the supernatant at 238nm and the concentration was calculated using the standard calibration curve.

The formula calculated drug loading;

Drug loading (%w/w) = weight of the drug in the formulation (mg) / total weight of formulation (mg) ×100

The formula calculated encapsulation efficiency;

EE (%) = amount of the drug in the formulation (mg)/theoretical drug loading (mg) × 100

Swelling study

The swelling of the beads was determined by immersing the beads in the various buffer media of pH 1.2, 6.8 and 7.4. The beads were removed after specific intervals to see the effect on the weight of the swelled beads. The formula calculated the weight change in the beads:

% weight change= (Ws - Wi/Wi) × 100

Ws is the weight of the beads after swelling and Wi is the weight of the beads at the start or initial weight.

The swelling of the beads was determined until an equilibrium weight of the beads was reached.

Each Wi contained not less than 0.01g of the beads.

Scanning electron microscopy

Shape, surface morphology, and the beads structure were validated using scanning electron microscopy (SEM) at the University of Agriculture, Faisalabad. The SEM images of formulations F0, F1 and F2 were analyzed by mounting them on the aluminum stubs using the two-sided adhesive tape (JEC-3000FC) coated with gold before scanning the beads. The images were captured at different voltages and different magnifications. The SEM images of the beads were obtained and then analyzed for shape, surface morphology and internal characterization.

Fourier transform infra-red spectroscopy

FTIR spectroscopy was used for interaction study to gain information about the functional group and any interaction between the drug and the polymers. The FTIR spectra of pure drug, chitosan, sodium alginate, blank formulation, and drug-loaded formulation were determined. The beads were blended in 1:100 proportion with potassium bromide and dried at 40^{o}C. The beads and potassium bromide mixture underwent a compression cycle by applying ten tons for two minutes. A 12mm transparent disc was used for the compression. Typically, the sample was scanned in the 400-4000/cm range using a Bruker Alpha spectrometer (Bruker Corporation). The characteristic peaks of IR spectra were reported for pure, blank, drug-loaded beads.

X-ray diffraction

To determine the drug-bead interaction and the physical state of LTZ, an XRD analysis of the drug and the formulation was acquired using an X-ray diffractometer (D8 Advance, Bruker). The patterns were obtained at room temperature at a current of 20mA and voltage of 35 kV.

Thermogravimetric analysis and differential scanning calorimetry

It was conducted to evaluate the drug's and the polymer's chemical structure, thermal weight loss and crystalline changes in the sample. For this purpose, the samples were heated under the atmosphere of nitrogen at the temperature range of 25-300^{o}C at a heating rate of 10^{o}C per minute on a DSC-60 (Shimadzu, Japan). The TGA was performed in the presence of the nitrogen with a flow rate of 20mL/minute and at a heating level of 10^{0}C/min using 2-3mg of sample.

In-vitro release kinetics of drug

The dissolution study was conducted employing the Type II dissolution apparatus (DT 70, Pharma Test, Germany), and the drug release was assessed for 24 hours. For this purpose 100mg of the beads were suspended in the dissolution media at 37±0.1ºC and the rotation speed was fixed at 100 rpm. The samples were taken at intervals of 0, 5, 15, 30, 45, 60, 90, 120 minutes until 24 hours. 5mL of the samples were removed and the equivalent volume was replaced with the same volume of fresh dissolution media. A membrane filter of pore size (0.45µm) was used to filter the sample before the analysis. All samples were examined using the UV-visible spectrophotometer, and the commutative drug release was calculated. The release kinetics data was further processed using DDSolver (version 1.0) to apply different release models.

Commulative drug release percentage vs time (Zero order plots)
Log commulative percent drug released vs time (First order)
Commulative percentage drug release vs time's square root (Higuchi plots)
Log commulative drug release percentage vs log time (Korsmeyer-Peppas plots)

STATISTICAL ANALYSIS

The statistical data analysis was performed using GraphPad Prism 5 (GraphPad Software Inc.; San Diego, CA, USA). All experiments were performed in triplicate, and the data are expressed as mean ± standard deviation (SD).

RESULTS

The particle size analysis of the beads suggested that when the CTS concentration increased, the size of the beads also increased (table 1). Similarly, the cumulative weight of the beads also increased as the chitosan concentration in the coagulation fluid was raised. However, the entrapment efficiency of the drug declined with increasing the chitosan concentration. There was high drug content in the beads containing more NaAlg contents. The beads entrapment efficiency ranged between 80.1% and 97.3%, depending on the concentration of chitosan and sodium alginate.

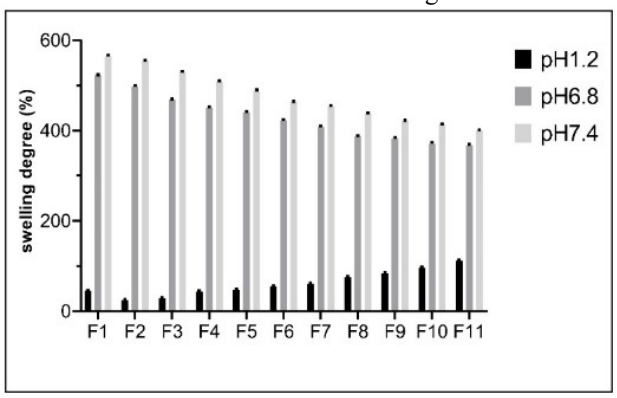

Fig. 1: Effect of pH on the swelling degree of dry Alg/CTS/LTZ beads. Data are mean ± SD (n=3).

The beads swelling was conducted in pH 1.2, 6.8 and 7.4, and the percentage weight changes were calculated. At pH 1.2, the beads were not significantly swelled, but a trend was seen according to which when the CTS concentration improved, the beads swelling also increased (fig. 1). However, the beads swell appreciably at the higher pH. A trend was seen in the swelling behaviour of the beads in the phosphate buffer of pH 6.8. The swelling degree was decreased as the chitosan concentration was increased and the alginate concentration in the beads was reduced. Almost the same pattern was shown in the swelling behaviour of the beads at pH 7.4.

Because the movement of water into the gel beads may be affected by the surface morphology of the hydrogel beads and the release kinetics of drugs, the shape of the beads was analysed by SEM. The SEM micrographs of different formulations (F0, F7, and F11) were obtained at 50x, 200x and 500x, keeping the potential at 7.0kv as conducted in a previous study (Gholamali and Yadollahi, 2020). The findings showed that the prepared beads were almost spherical, about 1.1-1.9mm in diameter, and had rough, irregular surfaces (fig. 2).

The results of FTIR analysis have been presented in fig. 3. The spectrum of hydrogel beads exhibited several characteristic bands. The broad peak observed at 3414 cm $^{-1}$ was correspond to newly formed intermolecular hydrogen-bonded O-H stretching and at 2250cm^{-1} for C-N stretching and other peaks were also seen from 500cm^{-1} to 1500cm^{-1} due to C-H bending in the CTS molecules. The absorption peaks between 1000cm^{-1} - 1400cm^{-1} can be assigned to the C=O stretching vibration and the peak at about 1650 was due to the N-acetyl group in chitosan. The characteristic peak at 1591cm^{-1} was due to C=O stretching vibration shifting to a higher wave number, 1606cm$^{-1,}$ for the ion cross-linking hydrogel.

It evinced the formation of ionic bonds between carboxylate ions of NaAlg and Ca^{2+} (Treenate and Monvisade, 2017). Furthermore, the characteristic peak at 1032cm^{-1} assigned to the C-O stretching vibration of NaAlg shifted to a higher wavenumber, 1056cm^{-1}. Based on the above analysis, it is proved that hydrogels formed because of multiple bonds between the two polymers. Besides, most of the peaks in the drug-loaded formulation overlapped with the pure drug absorption peaks, which means no strong chemical interaction occurred in the polymers and drug and the drug is only entrapped in matrices of polymers; there is no noticeable chemical interaction in drug and polymers.

XRD of the pure drug, chitosan, sodium alginate formulation F7 and F0 was characterized. The free drug exhibited sharp peaks, indicating its different crystalline form. In drug-loaded beads, no characteristic peak of the drug was found, corresponding to the amorphous nature of the drug (fig. 4). Furthermore, the semi crystalline structure of chitosan was interrupted during the formation of the beads. The DSC/TGA analysis of the beads is illustrated in fig. 5. The initial weight loss from 50-200^{o}C corresponds to the entrapped water molecules in the hydrogel network (fig. 5A-D). Differential scanning calorimetry was conducted on pure, chitosan, sodium alginate, drug-loaded and blank formulations.

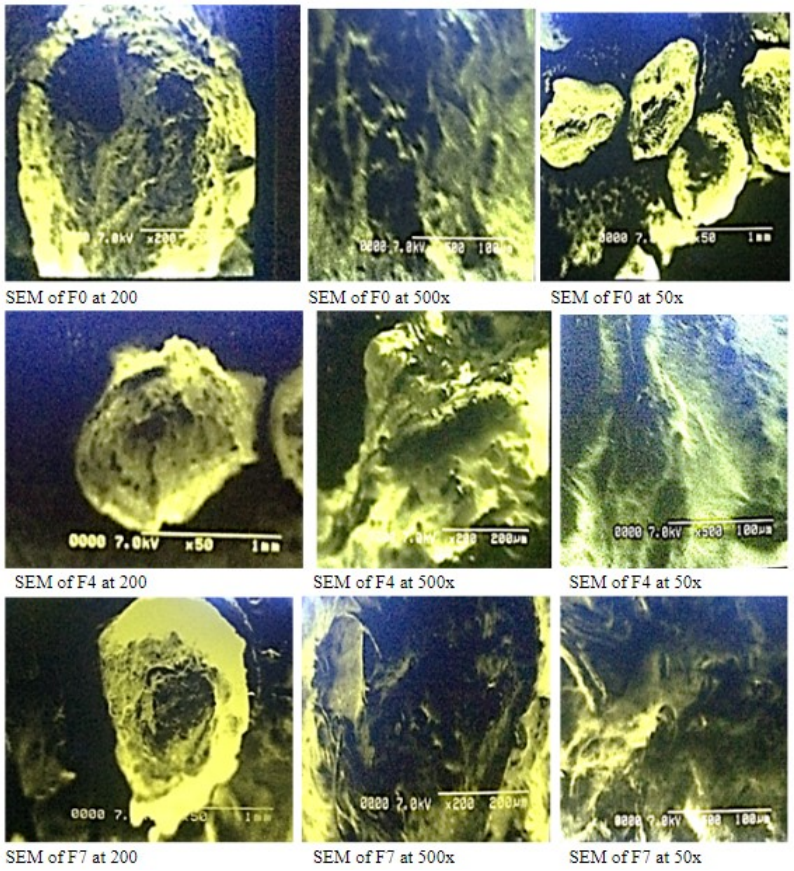

Fig. 2: shows SEM micrographs (50 x, 200k x, and 500x) of the hydrogel beads in dry condition.

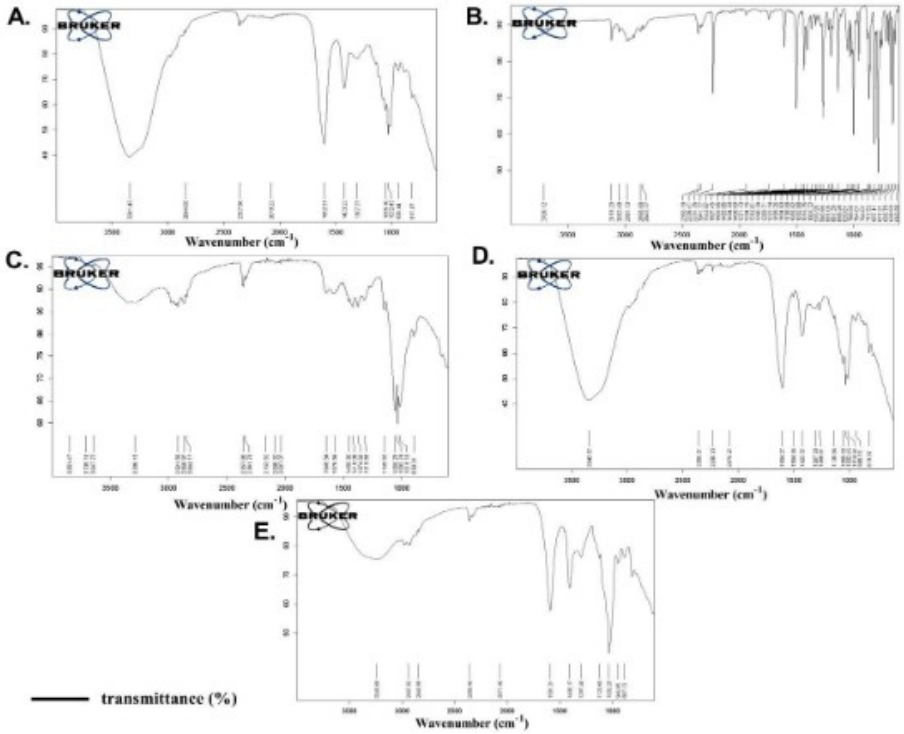

Fig. 3: FTIR spectra of (A) Drug-free blank beads, (B) free letrozole, (C) Chitosan only, (D) Drug-loaded beads and (E) sodium alginate only.

Table 1: The preparation of beads with consideration of size and EE% (for preparation of all the formulations, 10 mg dissolved drug, with 2% $CaCl_2$ was used), from F1 to F11, increasing concentration of chitosan was added for the optimization.

Formulation	CTS[b]	NaAlg [c]	Drug	Calcium chloride	EE[d]	Bead size (millimeter)	% yield
	(mg)	(mg)	(mg)	(%w/v)	%age	(Mean ± SD)	(w/w %)
F 0 (Blank)	60	940	0	2	0	0.87 ± 0.02	94.5
F1[a]	0	1000	10	2	97.3	1.11 ± 0.32	88.3
F2	10	990	10	2	94.2	1.32 ± 0.21	96.2
F3	20	980	10	2	93.8	1.34 ± 0.30	94.5
F4	30	970	10	2	91.7	1.56 ± 0.14	95.2
F5	40	960	10	2	90.1	1.67 ± 0.24	95.9
F6	50	950	10	2	88.5	1.69 ± 0.44	97.5
F7	60	940	10	2	86.9	1.59 ± 0.54	96.4
F8	70	930	10	2	84.4	1.66 ± 0.44	97.4
F9	80	920	10	2	83.1	1.86 ± 0.55	97.1
F10	90	910	10	2	81.8	1.89 ± 0.41	98.1
F11	100	900	10	2	80.1	1.97 ± 0.47	98.3

a. Letrozole, b. Chitosan, C. Sodium alginate, D. entrapment efficiency

Table 2: Correlation coefficients after the application of various models to the dissolution profile of letrozole-loaded beads (F1 to F11) using DD solver software.

Formulation code	Correlation coefficient (R^2)				
	Zero order	First order	Higuchi model	Korsemeyer-peppas model	Release exponent (n)
F1	-1.2410	0.9746	0.5134	0.9988	0.786
F2	-1.2410	0.9668	0.5134	0.9988	0.786
F3	-1.2410	0.9655	0.5134	0.9988	0.786
F4	-1.2410	0.9579	0.5134	0.9988	0.786
F5	-1.2410	0.9512	0.5134	0.9988	0.786
F6	-1.2410	0.9438	0.5134	0.9988	0.786
F7	-1.2410	0.9348	0.5134	0.9988	0.786
F8	-1.2410	0.9195	0.5134	0.9988	0.786
F9	-1.2410	0.9104	0.5134	0.9988	0.786
F10	-1.2410	0.9000	0.5134	0.9988	0.786
F11	-1.2410	0.8860	0.5134	0.9988	0.786

The thermogram of the letrozole showed an endothermic sharp peak at about 184°C, corresponding to its melting point. The drug-loaded formulation also showed a much broader peak at the same point, depicting the drug incorporated into the formulation.

The *in-vitro* release study at a slightly acidic pH (6.8) indicated that after the initial burst release, the drug escapes in a sustained fashion (fig. 6). Increasing the concentration of chitosan contents ensured a sustained drug release after a burst release. Thus, the release rate can be modified by changing the mixing ratios of NaAlg and CTS.

The release mechanism was further evaluated by comparing the correlation coefficient values obtained by putting the commutative percentage release of all formulations in several release models (zero order, first order, Higuchi and Korsemeyer, and Peppas models) (table 2). The correlation coefficient (R2) values depicted that prepared formulations followed the Korsemeyer and Peppas model with the R^2 values of 0.9988 for all the formulations and the release exponent (n) value was 0.786, respectively. The value of exponent n is more than 0.5 and less than 1, that is 0.786, which depicts the release was anomalous or nonfickian diffusion and the prepared drug delivery system was a dissolution and diffusion-controlled release system.

DISCUSSION

The beads were prepared by the ionotropic gelation method using different concentrations of polymers as prepared in an earlier study (Feyissa *et al.,* , 2023). A chitosan and sodium alginate blend was formulated whereas $CaCl_2$ was used as a gelating agent. The size of

the beads increased as the CTS concentration was increased. It might happen due to the formation of a thick chitosan layer in the beads and hence resists the formation of interfaces during bead formation. Similar observation of increasing the particle size with the increase of chitosan's amount has been observed in a former study (Wu *et al.,* 2020). It also indicates that the cross-linking network of sodium alginate is more compact than the cross-linking network of chitosan. Electrostatic interactions between the Ca^{2+} ions and the anionic alginate carbonyl ends (-COO-) ensures crosslinking of NaAlg chains, hence a gel forms (Khajuria *et al.,* 2020). Furthermore, cationic amino group ($-NH^{3+}$) of CS chain interacts via electrostatic interaction with the carbonyl ends of NaAlg, thus forming a dense network of intermolecular interactions. Besides, the decline of EE (%) with increasing CTS concentration may be due to the increase in contact and washing time when CTS was added, which has ensured that a portion of the drug was displaced from the gel to the aqueous phase.

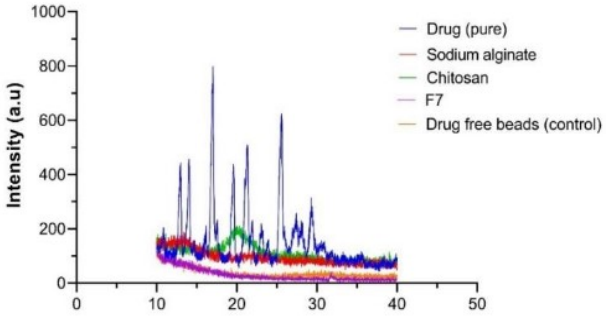

Fig. 4: The XRD spectra of pure drug, the polymers, drug-free and drug-loaded beads. The unit of the X-axis is 2 theta (degree).

The distinct variations in bead swelling ratios can be attributed to intermolecular non-covalent interactions, including ionic repulsion and hydrogen bonds. Furthermore, the degree of cross-linking may also influence the extent of swelling. The SEM images of the fabricated beads revealed a smooth surface. However, increased chitosan concentration made the surface rough, and the overall shape altered. As chitosan concentration increased, the appearance of a tail-like extension was observed. Beads with lower chitosan concentration displayed a smoother and more spherical morphology than those with higher ones. Such observations were also noticed in an earlier study (Wu *et al.,* 2020). This phenomenon could be attributed to the dehydration process during SEM sample preparation, which partially collapsed the polymeric network, consequently affecting the bead morphology.

The XRD analysis depicted the amorphous nature of the beads (fig. 4). It suggests a significant interaction between the drug and the polymers, attributed to hydrogen bonding between letrozole and the polymers. These hydrogen bonds likely formed due to interactions between the nitrogen atoms in letrozole and the hydrogen atoms of the hydroxyl (OH), ammonium (NH3+), and amino (NH_2) groups in the hydrogel beads. A reduction in the intensity of peaks in the beads suggests a limited interaction between the drug and the polymers, which retains the drug within the polymer matrices.

These findings indicate that the drug is entrapped within the polymeric structure, resulting in a less crystalline drug lattice within the polymer matrix, rendering it amorphous. The results revealed a homogeneous distribution of the drug within the polymeric matrices of the beads, a crucial criterion for an optimal drug delivery system.

The FTIR analysis demonstrated characteristic peaks at 1596 cm^{-1}, indicating stretching of the (COO-) group in sodium alginate, observed in the blank and drug-loaded formulations. Additionally, the peak at 2250 cm^{-1} was present in the drug-loaded formulation, signifying the C-N stretching vibration, absent in the blank formulation, and confirming the presence of letrozole in the loaded formulation. Most peaks in the drug-loaded formulation overlapped with the absorption peaks of the pure drug, suggesting that no substantial chemical interaction occurred between the polymers and the drug. Furthermore, the drug was solely entrapped within the polymer matrices without undergoing significant chemical changes.

The DSC and TGA results confirmed that the drug was crystalline. However, upon incorporation into the polymeric matrix, the drug became amorphous, as evidenced by the broader peak (Alemrayat *et al.,* 2019). This transformation to an amorphous form was more thermally stable than the crystalline form. Thermal characterization was performed on the drug-loaded, blank, pure drug, and polymers.

The TGA graph of the drug exhibited an initial mass loss in the temperature range of 50 to 200°C, followed by a sharp mass loss between 280°C and 350°C. Comparatively, the mass loss in the drug-loaded formulation was notably slower than in the blank formulation. This difference in mass loss rates can be attributed to the higher melting point of the polymers, chitosan and sodium alginate, compared to letrozole. Consequently, the drug-loaded and blank formulations displayed a slower mass loss profile, indicating increased stability of the prepared beads under heating conditions.

The release experiment demonstrated that a higher concentration of CTS reduced the initial rapid release of the drug from the beads, leading to a more controlled release pattern. This effect can be attributed to increasing the degree of ionic interaction and crosslinking between NaAlg and CS, thus resulting in more rigid network. Thus, it ensures a sustain release of the hydrophobic drug

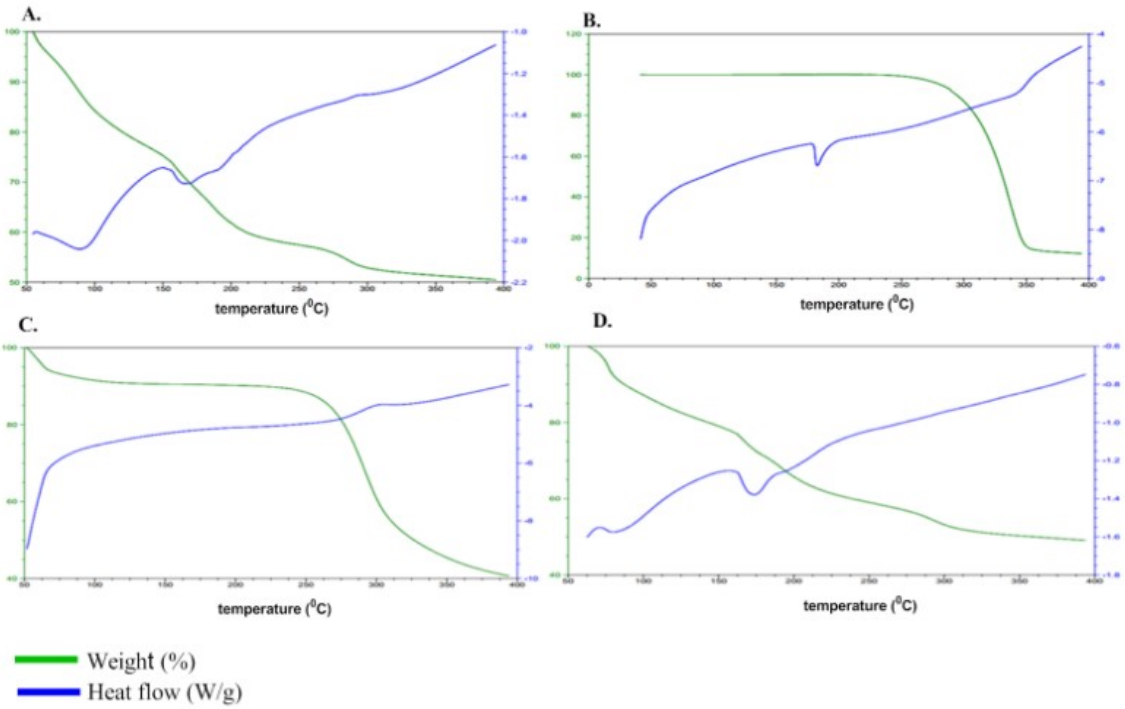

Fig. 5: DSC thermogram and TGA graph of (A) Drug-free blank beads (B) free drug (C) Chitosan only and (D) Drug loaded beads.

from the network (Feyissa *et al.,* 2023). Furthermore, the initial burst release may be attributed to the release of drug molecules adhered to the surface of the excipients, followed by a gradual release from the interior of the beads. The release pattern exhibited anomalous behavior, involving multiple release patterns, owing to the presence of two polymers uniformly blended in the system. One of the polymers, NaAlg, is hydrophilic and soluble in water, resulting in the early release of the drug through water solubilization and following a zero-order kinetic release. The other polymer, chitosan, is hydrophobic and retards the release of the hydrophobic drug, leading to later-stage release through diffusion, thereby achieving a controlled release pattern. In this manner, drug release from the beads followed multiple release patterns, rendering the delivery system anomalous and non-Fickian in nature.

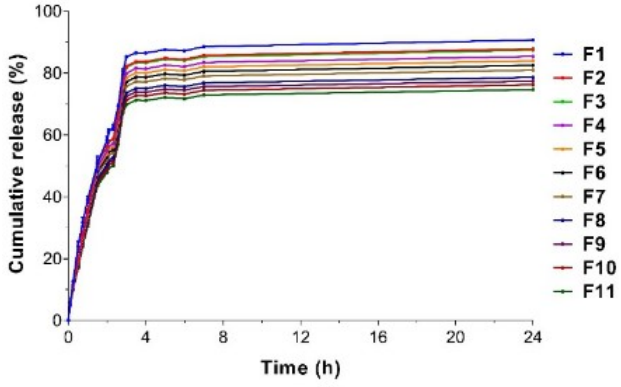

Fig. 6: *In-vitro* release behavior of letrozole from polymeric beads in PBS, pH 6.8.

CONCLUSION

Letrozole-loaded polymeric beads were successfully prepared by the ionotropic gelation method. Characteristics like swelling and release of drugs from polymeric beads were found to be pH sensitive. The FTIR, SEM, DSC and TGA analysis suggest that the entrapped drug is in amorphous form, and a minimum interaction exists between the drug and the excipients. *In vitro* LTZ release studies exhibited that the liberation of the drug is in direct proportion to the swelling of the beads. Kinetic modeling explained that all prepared beads followed more than one release pattern system, anomalous-non fickian. Hence, the results suggest that chitosan/sodium alginate bead can be used as potential carriers for the controlled release of letrozole for transcatheter arterial chemoembolization against breast cancer treatment, avoiding systemic effects while reducing the incidence of tumor relapse.

ACKNOWLEDGMENTS

We are grateful to the Faculty, Rashid Latif College of Pharmacy, for the insightful discussions, technical expertise and constructive feedback, which significantly enriched the quality of this work. We thank the Department of Pharmaceutics, Faculty of Pharmaceutical Sciences, Government College University, Faisalabad, Pakistan, for providing access to research facilities, library resources, and an academic environment.

REFERENCES

Alemrayat B, Elhissi A and Younes HM (2019). Preparation and characterization of letrozole-loaded poly (d, l-lactide) nanoparticles for drug delivery in breast cancer therapy. *Pharm. Dev. Techno.*, **24**(2): 235-242.

Bailleux C, Eberst L and Bachelot T (2021). Treatment strategies for breast cancer brain metastases. *BJC.*, **124**(1): 142-155.

Bialik-Wąs K, Królicka E and Malina D (2021). Impact of the type of crosslinking agents on the properties of modified sodium alginate/poly (vinyl alcohol) hydrogels. *Mol.*, **26**(8): 2381.

Boedtkjer E and Pedersen SF (2020). The acidic tumor microenvironment as a driver of cancer. *Annu. Rev, Physiol.*, **82**: 103-126.

Che Nan NF, Zainuddin N and Ahmad M (2019). Preparation and Swelling Study of CMC Hydrogel as Potential Superabsorbent. *Pertanika J. Sci. & Technol.*, **27**(1): 489-498.

Daniel S (2021). Biodegradable polymeric materials for medicinal applications. *Green Composites*, pp.351-372.

Feyissa ZG, Edossa D, Gupta NK and Negera D (2023). Development of double crosslinked sodium alginate/chitosan based hydrogels for controlled release of metronidazole and its antibacterial activity. *Heliyon*, **9**(9): e20144.

Gholamali I and Yadollahi M (2020). Doxorubicin-loaded carboxymethyl cellulose/Starch/ZnO nanocomposite hydrogel beads as an anticancer drug carrier agent. *Int. J. Biol. Macromol.*, **160**(3-4): 724-735.

Gnant M, Fitzal F, Rinnerthaler G, Steger GG, Greil-Ressler S, Balic M, Heck D, Jakesz R, Thaler J and Egle D (2021). Duration of adjuvant aromatase-inhibitor therapy in postmenopausal breast cancer. *NEJM*, **385**(5): 395-405.

Hakan A, Daltaban I and Vural S (2019). The role of temporal lobectomy as a part of surgical resuscitation in patients with severe traumatic brain injury. *Asian J. Neurosurg.*, **14**(02): 436-439.

Hosonaga M, Saya H and Arima Y (2020). Molecular and cellular mechanisms underlying brain metastasis of breast cancer. *Cancer Metastasis Rev.*, **39**(3): 711-720.

Kennoki N, Hori S, Yuki T and Hori A (2017). Transcatheter arterial chemoembolization with spherical embolic agent in patients with pulmonary or mediastinal metastases from breast cancer. *JVIR*, **28**(10): 1386-1394.

Khajuria DK, Vasireddi R, Priydarshi MK and Mahapatra DR (2020). Ionic diffusion and drug release behavior of core–shell-functionalized alginate–chitosan-based hydrogel. *ACS Omega,* **5**(1): 758-765.

Kim HJ, Cha SI, Kim CH, Lee J, Cho JY, Lee Y, Kim GJ and Lee DH (2019). Risk factors of postoperative acute lung injury following lobectomy for nonsmall cell lung cancer. *Medicine*, **98**(13): 1-6.

Luca A, Nacu I, Tanasache S, Peptu CA, Butnaru M and Verestiuc L (2023). New methacrylated biopolymer-based hydrogels as localized drug delivery systems in skin cancer therapy. *Gels*, **9**(5): 371.

Lv S, Zhang S, Zuo J, Liang S, Yang J, Wang J and Wei D (2023). Progress in preparation and properties of chitosan-based hydrogels. *Int. J. Biol. Macromol.,* **242**(2): 124915.

Nieto C, Vega MA, Rodríguez V, Pérez-Esteban P and Del Valle EMM (2022). Biodegradable gellan gum hydrogels loaded with paclitaxel for HER2+ breast cancer local therapy. *Carbohydr. Polym.*, **294**: 119732.

Qureshi MA, Nishat N, Jadoun S and Ansari MZ (2020). Polysaccharide based superabsorbent hydrogels and their methods of synthesis: A review. *Carbohydr. Polym. Technol. Appl.*, **1**: 100014.

Shao Z, Liu X, Peng C, Wang L and Xu D (2021). Combination of transcatheter arterial chemoembolization and portal vein embolization for patients with hepatocellular carcinoma: A review. *World J. Surg. Onc.*, **19**: 1-9.

Skolakova T, Slamova M, Skolakova A, Kaderabkova A, Patera J and Zámostny P (2019). Investigation of dissolution mechanism and release kinetics of poorly water-soluble tadalafil from amorphous solid dispersions prepared by various methods. *Pharmaceutics*, **11**(8): 383.

Song R, Murphy M, Li C, Ting K, Soo C and Zheng Z (2018). Current development of biodegradable polymeric materials for biomedical applications. *Drug Des Devel Ther.*, pp.3117-3145.

Sood A, Lang DK, Kaur R, Saini B and Arora S (2021). Relevance of aromatase inhibitors in breast cancer treatment. *Curr. Top Med. Chem.*, **21**(15): 1319-1336.

Treenate P and Monvisade P (2017). Crosslinker effects on properties of hydroxyethylacryl chitosan/sodium alginate hydrogel films. *Macromol. Symp*., **372**(1): 147-153.

Tuan Mohamood NF aZ, Abdul Halim AH and Zainuddin N (2021). Carboxymethyl cellulose hydrogel from biomass waste of oil palm empty fruit bunch using calcium chloride as crosslinking agent. *Polymers*, **13**(23): 4056.

Wu T, Yu S, Lin D, Wu Z, Xu J, Zhang J, Ding Z, Miao Y, Liu T, Chen T and Cai X (2020). Preparation, characterization, and release behavior of doxorubicin hydrochloride from dual cross-linked chitosan/alginate hydrogel beads. *ACS Appl. Bio Mater.,* **3**(5): 3057-3065.

Yetisgin AA, Cetinel S, Zuvin M, Kosar A and Kutlu O (2020). Therapeutic nanoparticles and their targeted delivery applications. *Molecules*, **25**(9): 2193.

Zaidi Z and Cherif MH (2019). The worldwide female breast cancer incidence and survival, 2018. *Pan Arab. J. Onc.*, **12**(2): 4191.